R. & M. No. 3325

MINISTRY OF AVIATION

AERONAUTICAL RESEARCH COUNCIL
REPORTS AND MEMORANDA

The Bending under Normal Loading of Plates Tapered in Planform

By G. G. Pope, M.Sc.(Eng.)

LONDON: HER MAJESTY'S STATIONERY OFFICE
1963
NINE SHILLINGS NET

The Bending under Normal Loading of Plates Tapered in Planform

By G. G. Pope, M.Sc.(Eng.)

Communicated by the Deputy Controller Aircraft (Research and Development), Ministry of Aviation

*Reports and Memoranda No. 3325**

April, 1962

Summary.

An analysis is given of the deformation under normal loading of a plate tapered symmetrically in planform with edges either clamped or simply-supported. The thickness may be constant or may vary along the plate as a power of the width. Numerical results are given for plates of constant and linearly varying thickness under uniformly distributed load.

1. *Introduction.*

An approximate analysis is given in this report of the small-deflection deformation under normal loading of a thin elastic plate tapered symmetrically in planform with edges either clamped or simply-supported. The thickness of the plate may be constant or may vary in the direction of taper as any power of the width.

The analysis is applicable to loadings under which the deflected shape across the plate normal to the direction of taper may be represented adequately anywhere along the plate in terms of a few known functions. The deflection of the plate can then be expressed in terms of the sum of the products of each of these functions with unknown functions representing the deflected shape in the direction of taper. Linear homogeneous differential equations are derived for these functions using the Rayleigh-Ritz method[2] and closed-form solutions are obtained. Similar solutions for rectangular plates of constant thickness have previously been obtained by Kantorovich[1]. The amount of computation increases rapidly with the number of functions used, and in the applications given here two functions only are used to represent the deflected shape across the plate.

If the shape of the load distribution across the plate does not vary and if the load intensity varies as a power of the width, it is shown that for a long plate (length/maximum width greater than about 2) an 'optimum' thickness variation can be derived in which the stress distribution on the surface does not vary along the plate except near the ends.

Williams[3] has examined the local bending behaviour of the corners of plates and has shown that infinite stresses are produced in theory at obtuse corners joining simply-supported edges. The

* Replaces R.A.E. Report No. Structures 273—A.R.C. 23,975.

present analysis is therefore not valid in the immediate vicinity of such corners. A similar singularity at corners joining simply-supported and clamped edges only occurs when the included angle exceeds 129°, which is larger than would be met in this context.

The general analysis is illustrated by application to a plate under uniformly distributed loading with the same boundary conditions along opposite edges. All such combinations are considered in turn. The deflected shape across the plate is here represented by the deflected shape across a parallel infinite strip under the same loading and boundary conditions, together with a second polynomial of higher power. It is shown that in this example an analysis using the first function alone, which could easily be performed on a desk calculating machine, will often give adequate results even for the maximum stress in the plate. Curves showing the variation with the plate geometry of the maximum deflection and the maximum value of the von Mises stress away from the corners are given both for a plate of constant thickness and for a linear thickness variation, the latter being the 'optimum' thickness variation for this loading.

2. *Analysis.*

2.1. *Basic Theory.*

2.1.1. *Some general results.*—The strain energy of bending U of a thin plate in the x, y plane undergoing a small lateral deflection $w(x, y)$ is given by the expression[2]

$$U = \frac{1}{2}\int\int D\left\{(\nabla^2 w)^2 - 2(1-\nu)\left[\frac{\partial^2 w}{\partial x^2}\frac{\partial^2 w}{\partial y^2} - \left(\frac{\partial^2 w}{\partial x\,\partial y}\right)^2\right]\right\} dx\,dy.$$

The increment of the strain energy due to an infinitesimal arbitrary variation δw of the deflection is thus

$$\delta U = \int\int D\left\{\nabla^2 w \nabla^2(\delta w) - (1-\nu)\left[\frac{\partial^2 w}{\partial x^2}\frac{\partial^2 \delta w}{\partial y^2} + \frac{\partial^2 \delta w}{\partial x^2}\frac{\partial^2 w}{\partial y^2} - 2\frac{\partial^2 w}{\partial x\,\partial y}\frac{\partial^2 \delta w}{\partial x\,\partial y}\right]\right\} dx\,dy. \quad (1)$$

Moreover, provided the total work done on the edges of the plate by the variation δw is zero, and provided the flexural rigidity D is a function of x only, the following expression can be obtained by integrating equation (1) twice by parts.

$$\delta U = \int\int \delta w\left[D\nabla^4 w + 2\frac{dD}{dx}\frac{\partial}{\partial x}(\nabla^2 w) + \frac{d^2 D}{dx^2}\left(\frac{\partial^2 w}{\partial x^2} + \nu\frac{\partial^2 w}{\partial y^2}\right)\right] dx\,dy. \quad (2)$$

The line integrals around the edges of the plate which arise in the process of integrating by parts correspond to work done by forces or moments acting on the edges and here vanish due to the restrictions imposed on δw.

The work done on the plate due to the variation δw of the displacement is given by

$$\delta T = \int\int q(x, y)\delta w\,dx\,dy \quad (3)$$

where $q(x, y)$ is the distributed load.

Now, by the principle of virtual displacements, the total work done by the infinitesimal variation of the displacements is equal to the change in the strain energy, so that

$$\delta T = \delta U.$$

Hence equating expressions (2) and (3), we obtain

$$\iint \delta w \left[D\nabla^4 w + 2\frac{dD}{dx}\frac{\partial}{\partial x}(\nabla^2 w) + \frac{d^2D}{dx^2}\left(\frac{\partial^2 w}{\partial x^2} + \nu\frac{\partial^2 w}{\partial y^2}\right) - q(x, y)\right] dx\, dy = 0. \qquad (4)$$

If the variation δw were completely arbitrary within the plate, equation (4) would yield the exact equation for the bending of the plate. In the present problem however an approximate solution is found by considering only a restricted variation of w.

2.1.2. *Application to tapered plates.*—The axes and notation used here are shown in Fig. 1. The plate is symmetrically positioned relative to the x axis, the parallel ends being defined by the lines $x = 0$ and $x = a$. It is convenient to express the problem in terms of the following non-dimensional symbols

$$W = \frac{w}{a}, \qquad X = 1 + \rho\frac{x}{a}, \qquad Y = \frac{2y}{b_1},$$

$$\theta = \frac{Y}{X}, \qquad \rho = \frac{b_2}{b_1} - 1, \qquad \mu = \frac{a}{b_1}.$$

The symbols b_1 and b_2 represent the widths of the plate at $x = 0$ and $x = a$ respectively ($b_1 > b_2$). The co-ordinate X represents in non-dimensional form the distance along the plate measured from the point at which the sides would meet if produced.

The analysis given here is immediately applicable when the shape of the load distribution across the plate does not vary along the plate. More complicated problems may be considered by adding together a number of such load distributions, which can each be expressed in the form

$$q = q_0\alpha(X)\beta(\theta)$$

where q_0 is a constant and the functions α and β express the shape of the load distribution.

The most general variation of the flexural rigidity to which this analysis is applicable can be expressed in the form

$$D = D_1 X^r$$

where D_1 and r are constants.

Re-expressing equation (4) in the notation of this section, we obtain

$$\iint D\delta W \left[\rho^4\frac{\partial^4 W}{\partial X^4} + 8\rho^2\mu^2\frac{\partial^4 W}{\partial X^2\partial Y^2} + 16\mu^4\frac{\partial^4 W}{\partial Y^4} + \frac{2r\rho^2}{X}\frac{\partial}{\partial X}\left(\rho^2\frac{\partial^2 W}{\partial X^2} + 4\mu^2\frac{\partial^2 W}{\partial Y^2}\right) + \right.$$

$$\left. + \frac{r(r-1)\rho^2}{X^2}\left(\rho^2\frac{\partial^2 W}{\partial X^2} + 4\nu\mu^2\frac{\partial^2 W}{\partial Y^2}\right) - \frac{q_0 a^3\alpha(X)\beta(\theta)}{D_1 X^r}\right] dX\, dY = 0. \qquad (5)$$

An approximate solution is obtained to this equation by assuming that W can be expressed in the form

$$W = \sum_1^m f_j(X)\Phi_j(\theta) \qquad (6)$$

where the functions $\Phi_j(\theta)$ are chosen to represent approximately the deflected shape normal to the X axis and the functions $f_j(X)$ are unspecified. Simultaneous differential equations for these functions are obtained by substituting equation (6) in equation (5) and considering in turn the following m restricted variations of W.

$$\delta W_j = \Phi_j \delta f_j. \qquad (7)$$

The integration sign with respect to X may then be removed from equation (5) because the variations δf_j are completely arbitrary within the plate. If the resulting equations are then divided through by the relevant variations δf_j and integrated with respect to θ, the following set of equations is obtained.

$$\sum_{k=1}^{k=m}\left(\sum_{i=1}^{i=4} p_{jki}X^i\frac{d^i f_k}{dX^i}+p_{jk0}f_k\right)=\frac{12(1-\nu^2)\alpha\mu^3\Psi_j R}{X^{r-4}} \tag{8}$$

where

$$\Psi_j=\int_{-1}^{+1}\beta\Phi_j d\theta,\qquad R=\frac{q_0}{E}\left(\frac{b_1}{t_1}\right)^3,$$

$$\left.\begin{aligned}
p_{jk0} &= \rho^4\{l_{jk4}+12l_{jk3}+36l_{jk2}+24l_{jk1}-2r(l_{jk3}+6l_{jk2}+6l_{jk1})+\\
&\quad +r(r-1)(l_{jk2}+2l_{jk1})\}+4\rho^2\mu^2\{2(s_{jk2}+6s_{jk1}+6s_{jk0})-\\
&\quad -2r(s_{jk1}+2s_{jk0})+r(r-1)\nu s_{jk0}\}+16\mu^4 m_{jk},\\
p_{jk1} &= \rho^4\{-4(l_{jk3}+6l_{jk2}+6l_{jk1})+6r(l_{jk2}+2l_{jk1})-2r(r-1)l_{jk1}\}+\\
&\quad +4\rho^2\mu^2\{-4(s_{jk1}+2s_{jk0})+2rs_{jk0}\},\\
p_{jk2} &= \rho^4\{6(l_{jk2}+2l_{jk1})-6rl_{jk1}+r(r-1)l_{jk0}\}+8\rho^2\mu^2 s_{jk0},\\
p_{jk3} &= -2\rho^4(2l_{jk1}-rl_{jk0}),\\
p_{jk4} &= \rho^4 l_{jk0}
\end{aligned}\right\} \tag{9}$$

and

$$\left.\begin{aligned}
l_{jki} &= \int_{-1}^{+1}\theta^i\Phi_j\frac{d^i\Phi_k}{d\theta^i}d\theta, & l_{jk0} &= \int_{-1}^{+1}\Phi_j\Phi_k d\theta,\\
s_{jki} &= \int_{-1}^{+1}\theta^i\Phi_j\frac{d^{i+2}\Phi_k}{d\theta^{i+2}}d\theta, & m_{jk} &= \int_{-1}^{+1}\Phi_j\frac{d^4\Phi_k}{d\theta^4}d\theta.
\end{aligned}\right\} \tag{10}$$

2.1.3. *Solution of equations.*—As equations (8) are of linear and homogeneous form, they can be solved by standard methods. In the numerical examples given in this report two unknown functions only are considered. For simplicity of presentation the subsequent analysis is therefore restricted to assumed deflected shapes of the form

$$W=f_1(X)\Phi_1(\theta)+f_2(X)\Phi_2(\theta). \tag{11}$$

The complementary function of the solution to equations (8) is then found by substituting

$$f_1=AX^\lambda$$

$$f_2=BX^\lambda$$

and equating the left-hand sides of these equations to zero, giving

$$\left.\begin{aligned}
Ah_{11}(\lambda)+Bh_{12}(\lambda)&=0\\
\text{and}\qquad Ah_{12}(\lambda)+Bh_{22}(\lambda)&=0
\end{aligned}\right\} \tag{12}$$

where

$$h_{jk}(\gamma)=\gamma^4 p_{jk4}+\gamma^3(-6p_{jk4}+p_{jk3})+\gamma^2(11p_{jk4}-3p_{jk3}+p_{jk2})+$$
$$+\gamma(-6p_{jk4}+2p_{jk3}-p_{jk2}+p_{jk1})+p_{jk0}. \tag{13}$$

Equations (12) are only consistent if the determinant $\Delta(\lambda)$ of the coefficients of A and B is zero, that is

$$\Delta(\lambda) = h_{11}(\lambda)h_{22}(\lambda) - h_{12}(\lambda)h_{21}(\lambda) = 0.$$

The complete solution is then given by

$$\left.\begin{aligned} f_1 &= F_1(X) + \sum_{i=1}^{i=8} A_i X^{\lambda_i} \\ f_2 &= F_2(X) + \sum_{i=1}^{i=8} B_i X^{\lambda_i} \end{aligned}\right\} \tag{14}$$

where F_1 and F_2 are the relevant particular integrals and the constants A_i and B_i are related by the expression

$$\frac{B_i}{A_i} = -\frac{h_{11}(\lambda_i)}{h_{12}(\lambda_i)} = -\frac{h_{21}(\lambda_i)}{h_{22}(\lambda_i)}.$$

The eight arbitrary coefficients in the above complete solution can be found from the boundary conditions on each of the functions f_j at $X = 1$ and $X = 1 + \rho$. The constants A_i and B_i and the indices λ_i are in general complex.

If the load intensity at constant θ along the plate varies as X^v, the particular integrals in expressions (14) are given by

$$\left.\begin{aligned} F_1(X) &= \frac{12(1-\nu^2)\mu^3 R}{\Delta(4-r+v)} \{\Psi_1 h_{22}(4-r+v) - \Psi_2 h_{12}(4-r+v)\} X^{4-r+v} \\ F_2(X) &= \frac{12(1-\nu^2)\mu^3 R}{\Delta(4-r+v)} \{\Psi_2 h_{11}(4-r+v) - \Psi_1 h_{21}(4-r+v)\} X^{4-r+v} \end{aligned}\right\} \tag{15}$$

or, if only one function f is used in the analysis,

$$F(X) = \frac{12(1-\nu^2)\mu^3 R}{h(4-r+v)} \Psi X^{4-r+v}.$$

2.1.4. *Moments and stresses in plate.*—The bending moments M_x and M_y and the twisting moment M_{xy} are given by the expressions,

$$\left.\begin{aligned} M_x &= -D\left(\frac{\partial^2 w}{\partial x^2} + \nu \frac{\partial^2 w}{\partial y^2}\right) \\ &= -\frac{D_1 X^r}{\mu b_1}\left(\rho^2 \frac{\partial^2 W}{\partial X^2} + 4\nu\mu^2 \frac{\partial^2 W}{\partial Y^2}\right), \\ M_y &= -D\left(\frac{\partial^2 w}{\partial y^2} + \nu \frac{\partial^2 w}{\partial x^2}\right) \\ &= -\frac{D_1 X^r}{\mu b_1}\left(4\mu^2 \frac{\partial^2 W}{\partial Y^2} + \nu\rho^2 \frac{\partial^2 W}{\partial X^2}\right), \\ M_{xy} &= D(1-\nu)\frac{\partial^2 w}{\partial x\,\partial y} \\ &= 2\frac{D_1 X^r}{b_1}(1-\nu)\rho \frac{\partial^2 W}{\partial X\,\partial Y}. \end{aligned}\right\} \tag{16}$$

Substitution of the assumed deflected form (11) into the derivatives of W gives

$$\left.\begin{aligned}\frac{\partial^2 W}{\partial X^2} &= \sum_{j=1}^{j=2} \frac{1}{X^2}\left[\Phi_j X^2 f_j'' - 2\theta\Phi_j' X f_j' + \theta(\theta\Phi_j''+2\Phi_j')f_j\right],\\ \frac{\partial^2 W}{\partial X\,\partial Y} &= \sum_{j=1}^{j=2} \frac{1}{X^2}\left[\Phi_j' X f_j' - (\theta\Phi_j''+\Phi_j')f_j\right],\\ \frac{\partial^2 W}{\partial Y^2} &= \sum_{j=1}^{j=2} \frac{1}{X^2}\Phi_j'' f_j\end{aligned}\right\} \tag{17}$$

where $f_j' = \dfrac{df_j}{dX}$ and $\Phi_j' = \dfrac{d\Phi_j}{d\theta}$.

The value of the von Mises stress σ_f on the surface of the plate, which is here assumed to govern the yielding of the plate, is given by

$$\begin{aligned}\sigma_f &= \sqrt{(\sigma_x^2+\sigma_y^2-\sigma_x\sigma_y+3\tau_{xy}^2)}\\ &= \frac{6}{t_1^2 X^{2r/3}}\sqrt{(M_x^2+M_y^2-M_xM_y+3M_{xy}^2)}\end{aligned} \tag{18}$$

where t_1 is the thickness of the plate at $X = 1$.

2.1.5. *Boundary conditions.*

(i) *Boundary conditions at ends.*—The boundary condition of zero deflection at the ends of the plate is satisfied completely by making

$$[f_j]_{\text{end}} = [\delta f_j]_{\text{end}} = 0. \tag{19}$$

The further condition necessary for the virtual displacement δW_j to do no work on the ends is given by

$$\left[\int_{-1}^{+1} \frac{\partial \delta W_j}{\partial X}\left(\rho^2 \frac{\partial^2 W}{\partial X^2} + 4\nu\mu^2 \frac{\partial^2 W}{\partial Y^2}\right) d\theta\right]_{\text{end}} = 0. \tag{20}$$

Substituting equations (17) and (19) in equation (20), we obtain

$$\left[\delta f_j'\rho^2 \sum_{k=1}^{k=2}\left(l_{jk0}f_k'' - \frac{2}{X}l_{jk1}f_k'\right)\right]_{\text{end}} = 0.$$

The second boundary condition for a clamped end is thus satisfied completely by making

$$[f_j']_{\text{end}} = [\delta f_j']_{\text{end}} = 0$$

and that for a simply-supported end is represented approximately by

$$\left[\sum_{k=1}^{k=2}\left(l_{jk0}f_k'' - \frac{2}{X}l_{jk1}f_k'\right)\right]_{\text{end}} = 0.$$

(ii) *Boundary conditions at clamped sides.*—The deflection functions Φ_j can be chosen to satisfy the boundary conditions along clamped sides completely. If a complete series of functions Φ_j were used and if the ends of the plate were also clamped this method would thus give a solution which would converge to the exact solution as the number of functions was increased.

(iii) *Boundary conditions at simply-supported sides.*—The boundary conditions cannot be satisfied purely by appropriate choice of the functions Φ_j if the sides are simply-supported,

because the expression for the bending moment about the sides also involves the unknown functions f_j. The deflected shape across the plate is here represented approximately by functions which would satisfy these boundary conditions completely if the sides were parallel. It can be shown[4] that the total work done on the sides of the plate in this deflected shape is zero if the plate thickness is constant and the derivation of equations (8) is then strictly valid. Errors introduced by using this derivation when the thickness varies should be small compared with those due directly to the moments along the sides which would be strictly necessary to maintain this deflected form irrespective of the thickness variation. These moments, which are illustrated for a specific example in Fig. 12, are usually small but can lead to inaccurate results for large angles of taper.

2.2. *Some Special Cases.*

2.2.1. *Plates of constant thickness.*—For a plate of constant thickness

$$r = 0$$

and the coefficients of equation (8) are given by

$$\begin{aligned}
p_{jk0} &= \rho^4(l_{jk4}+12l_{jk3}+36l_{jk2}+24l_{jk1}) + 8\rho^2\mu^2(s_{jk2}+6s_{jk1}+6s_{jk0}) + 16\mu^4 m_{jk},\\
p_{jk1} &= -4\rho^4(l_{jk3}+6l_{jk2}+6l_{jk1}) - 16\rho^2\mu^2(s_{jk1}+2s_{jk0}),\\
p_{jk2} &= 6\rho^4(l_{jk2}+2l_{jk1}) + 8\rho^2\mu^2 s_{jk0},\\
p_{jk3} &= -4\rho^4 l_{jk1},\\
p_{jk4} &= \rho^4 l_{jk0}.
\end{aligned}$$

2.2.2. *Optimum thickness variation when load at constant θ varies as X^v.*—The particular integrals given in equations (15) can be interpreted physically as representing the deflection of a semi-infinite tapered strip under the same loading with the relevant boundary conditions along the sides. To these are added the complementary functions which here represent the additional deflection necessary to make the strip satisfy the boundary conditions at the ends of the plate. Thus in a relatively long plate the influence of these complementary functions is only significant near the ends and elsewhere the plate behaves as a semi-infinite tapered strip. Now by substituting the particular integrals, equations (15), in equations (17) it is seen that for such a strip the second derivatives of W with respect to X and Y vary as X^{2+v-r}. Substituting these successively into equations (16) and (18), the von Mises stress σ_f is seen to vary as $X^{2+v-2r/3}$. Hence the optimum thickness variation of the semi-infinite strip in which the surface stresses at all chordwise sections are the same is given by

$$r = \frac{3}{2}(v+2).$$

Thus for a relatively long plate this represents a near optimum thickness variation.

3. *Application to Plates under Uniformly Distributed Loading.*

3.1. *Specific Examples Chosen.*

The preceding analysis has been computed for plates under uniform loading with opposite pairs of edges either clamped or simply-supported. The plate thickness is either constant or linearly proportional to the width, the latter being the optimum thickness variation for long plates in the sense described in Section 2.2.2.

The functions chosen to describe the deflected shape across the plate are given in Section 3.2 together with the constants and equations derived using them. In each case the first function chosen is the deflected shape across an infinitely long strip of constant thickness under uniform loading with the relevant boundary conditions. In long plates the influence of the second function is only significant near the ends and the computation of the two-function analysis becomes impracticable. Equations are given therefore both for one-function and for two-function analyses.

The figures plotted are listed in Section 3.3 and the results are discussed in Section 3.4.

3.2. *Transverse Deflection Functions and Related Constants.*

3.2.1. *Plate with clamped sides.*—The transverse deflection functions are chosen as

$$\Phi_1 = \theta^4 - 2\theta^2 + 1,$$

$$\Phi_2 = \theta^2(\theta^4 - 2\theta^2 + 1).$$

The related constants are shown in the following tables:

i	$315l_{11i}$	$3465l_{12i}$	$3465l_{21i}$	$45045l_{22i}$
0	+ 256	+ 256	+ 256	+ 768
1	− 128	+ 128	− 384	− 384
2	0	− 768	+ 256	− 3584
3	+ 384	+ 1152	+ 1920	+ 17280
4	+ 384	+ 20352	+ 1920	+ 151680

i	$105s_{11i}$	$315s_{12i}$	$315s_{21i}$	$3465s_{22i}$
0	− 256	0	0	− 768
1	+ 384	− 384	+ 384	+ 1152
2	+ 384	+ 3456	+ 384	+ 20352

$5m_{11}$	$35m_{12}$	$35m_{21}$	$315m_{22}$
128	128	128	3456

$15\Phi_1$	$105\Phi_2$
16	16

Substituting in equations (8), the following equations are obtained for f_1 and f_2.

(i) *Plate of constant thickness.*

(*a*) Single-function analysis.

$$3(5\rho^4 + 72\rho^2\mu^2 + 336\mu^4)f + 12\rho^2(\rho^2 + 4\mu^2)(Xf' - X^2f'') + 2\rho^4(2X^3f''' + X^4f'''') = 28\cdot665\mu^3RX^4$$

where a dash denotes differentiation with respect to X and $\nu = 0\cdot3$.

(*b*) Two-function analysis.

$$33(5\rho^4+72\rho^2\mu^2+336\mu^4)f_1+132\rho^2(\rho^2+4\mu^2)(Xf_1'-X^2f_1'')+$$
$$+22\rho^4(2X^3f_1'''+X^4f_1'''')+3(25\rho^4+264\rho^2\mu^2+528\mu^4)f_2+$$
$$+12\rho^2(7\rho^2+44\mu^2)Xf_2'-2\rho^4(12X^2f_2''+2X^3f_2'''-X^4f_2'''')=315\cdot315\mu^3RX^4,$$

$$39(65\rho^4+616\rho^2\mu^2+528\mu^4)f_1-156\rho^2(3\rho^2+44\mu^2)Xf_1'-2\rho^4(156X^2f_1''-$$
$$-78X^3f_1'''-13X^4f_1'''')+(1725\rho^4+18408\rho^2\mu^2+61776\mu^4)f_2+$$
$$+4\rho^2(51\rho^2+156\mu^2)Xf_2'-4\rho^2(51\rho^2+156\mu^2)X^2f_2''+6\rho^4(2X^3f_2'''+X^4f_2'''')$$
$$=585\cdot585\mu^3RX^4.$$

(ii) *Plate with thickness proportional to width.*

(*a*) Single-function analysis.

$$(21\rho^4+244\cdot8\rho^2\mu^2+1008\mu^4)f-12\rho^2(\rho^2+8\mu^2)Xf'+6\rho^2(3\rho^2-8\mu^2)X^2f''+$$
$$+2\rho^4(8X^3f'''+X^4f'''')=28\cdot665\mu^3RX.$$

(*b*) Two-function analysis.

$$11(21\rho^4+244\cdot8\rho^2\mu^2+1008\mu^4)f_1-132\rho^2(\rho^2+8\mu^2)Xf_1+66\rho^2(3\rho^2-8\mu^2)X^2f_1''+$$
$$+22\rho^4(8X^3f_1'''+X^4f_1'''')+(177\rho^4+1584\rho^2\mu^2+1584\mu^4)f_2+528\rho^2\mu^2Xf_2'-$$
$$-2\rho^4(15X^2f_2''-4X^3f_2'''-X^4f_2'''')=315\cdot315\mu^3RX,$$

$$13(117\rho^4+1056\rho^2\mu^2+1584\mu^4)f_1-312\rho^2(3\rho^2+22\mu^2)Xf_1'+26\rho^4(21X^2f_1''+$$
$$+12X^3f_1'''+X^4f_1'''')+(1827\rho^4+18782\cdot4\rho^2\mu^2+61776\mu^4)f_2-12\rho^2(31\rho^2+104\mu^2)Xf_2'-$$
$$-2\rho^2(57\rho^2+312\mu^2)X^2f_2''+6\rho^4(8X^3f_2'''+X^4f_2'''')=585\cdot585\mu^3RX.$$

3.2.2. *Plate with simply-supported sides.*—The transverse deflection functions are chosen as

$$\Phi_1=\theta^4-6\theta^2+5,$$
$$\Phi_2=\theta^2(5\theta^4-14\theta^2+9).$$

The related constants are shown in the following tables:

i	$315l_{11i}$	$3465l_{12i}$	$3465l_{21i}$	$45045l_{22i}$
0	+ 7936	+ 18176	+ 18176	+ 105728
1	− 3968	+ 6272	− 24448	− 51840
2	− 2688	− 75648	− 14208	− 706944
3	+ 3840	− 15360	+ 30720	+ 456960
4	+ 3840	+ 1136640	+ 30720	+12552960

i	$35s_{11i}$	$315s_{12i}$	$315s_{21i}$	$3465s_{22i}$
0	− 2176	− 4224	− 4224	− 107904
1	+ 1024	− 33024	+ 5376	− 59904
2	+ 1024	+ 158976	+ 5376	+ 1476096

$5m_{11}$	$35m_{12}$	$35m_{21}$	$315m_{22}$
768	1536	1536	209664

$5\Psi_1$	$35\Psi_2$
32	64

Substituting in equations (8), the following equations are obtained for f_1 and f_2.

(i) *Plate of constant thickness.*

(*a*) Single-function analysis.

$$3(-185\rho^4-552\rho^2\mu^2+1008\mu^4)f+12\rho^2(47\rho^2+156\mu^2)Xf'-$$
$$-3\rho^2(83\rho^2+204\mu^2)X^2f''+31\rho^4(2X^3f'''+X^4f'''')=85\cdot995\mu^3RX^4.$$

(*b*) Two-function analysis.

$$33(-185\rho^4-552\rho^2\mu^2+1008\mu^4)f_1+132\rho^2(47\rho^2+156\mu^2)Xf_1'-$$
$$-33\rho^2(83\rho^2+204\mu^2)X^2f_1''+341\rho^4(2X^3f_1'''+X^4f_1'''')-6(1055\rho^4+$$
$$+3696\rho^2\mu^2-1584\mu^4)f_2+24\rho^2(281\rho^2+1188\mu^2)Xf_2'-3\rho^2(493\rho^2+484\mu^2)X^2f_2''-$$
$$-\rho^4(98X^3f_2'''-71X^4f_2'''')=945\cdot945\mu^3RX^4,$$

$$78(-455\rho^4+704\rho^2\mu^2+1584\mu^4)f_1+312\rho^2(131\rho^2+88\mu^2)Xf_1'-$$
$$-39\rho^2(493\rho^2+484\mu^2)X^2f_1''+\rho^4(4966X^3f_1'''+923X^4f_1'''')+$$
$$+3(-11273\rho^4+63544\rho^2\mu^2+624624\mu^4)f_2+12\rho^2(5333\rho^2+18668\mu^2)Xf_2'-$$
$$-3\rho^2(6333\rho^2+14612\mu^2)X^2f_2''+\rho^4(810X^3f_2'''+413X^4f_2'''')=3513\cdot51\mu^3RX^4.$$

(ii) *Plate with thickness proportional to width.*

(*a*) Single-function analysis.

$$(42\rho^4+601\cdot2\rho^2\mu^2+3024\mu^4)f+3\rho^2(\rho^2+12\mu^2)Xf'+$$
$$+4\rho^2(54\rho^2-153\mu^2)X^2f''+31\rho^4(8X^3f'''+X^4f'''')=85\cdot995\mu^3RX.$$

(*b*) Two-function analysis.

$$11(42\rho^4+601\cdot2\rho^2\mu^2+3024\mu^4)f_1+33\rho^2(\rho^2+12\mu^2)Xf_1'+44\rho^2(54\rho^2-153\mu^2)X^2f_1''+$$
$$+341\rho^4(8X^3f_1'''+X^4f_1'''')+(2307\rho^4+19285\cdot2\rho^2\mu^2+9504\mu^4)f_2+$$
$$+\rho^2(2013\rho^2+24156\mu^2)Xf_2'-\rho^2(1494\rho^2+1452\mu^2)X^2f_2''+\rho^4(328X^3f_2'''+71X^4f_2'''')$$
$$=945\cdot945\mu^3RX,$$

$$13(507\rho^4+6085\cdot2\rho^2\mu^2+9504\mu^4)f_1-39\rho^2(49\rho^2+748\mu^2)Xf_1'+$$
$$+78\rho^2(111\rho^2-242\mu^2)X^2f_1''+13\rho^4(X^3f_1'''+X^4f_1'''')+$$
$$+(43176\rho^4+487203\cdot6\rho^2\mu^2+1873872\mu^4)f_2+3\rho^2(3143\rho^2+30836\mu^2)Xf_2'-$$
$$-12\rho^2(1073\rho^2+3653\mu^2)X^2f_2''+\rho^4(3288X^3f_2'''+413X^4f_2'''')=3513\cdot51\mu^3RX.$$

3.3. *Results.*

The variations of the maximum deflection and the maximum value of the von Mises stress σ_f with a/b_1 are plotted in the figures listed below for a series of values of b_1/b_2. The corresponding curves for rectangular plates which are also given in these figures have been obtained from results given by Timoshenko and Woinowsky-Krieger[2].

Thickness	Boundary conditions		Maximum σ_f occurs on ($a/b_1 > 1$)	Fig. No.
	Sides	Ends		
Constant	Clamped	Clamped	Sides	2
	Clamped	Simply-supported	Sides	3
	Simply-supported	Clamped	Wide end	4
	Simply-supported	Simply-supported	Centre-line*	5
Proportional to width	Clamped	Clamped	Sides	6
	Clamped	Simply-supported	Sides	7
	Simply-supported	Clamped	Narrow end	8
	Simply-supported	Simply-supported	Centre-line*	9

* large bending stresses in the immediate vicinity of the obtuse corners are neglected.

The following examples are plotted in more detail. The deflection w and the von Mises stress σ_f are plotted in each case along the centre-line of the plate. The von Mises stress along the clamped sides and the error bending stress normal to the simply-supported sides are also plotted.

Fig. 10. Comparison of specimen results of the two analyses. Sides and ends clamped, thickness constant, $a/b_1 = 2$, $b_2/b_1 = 0{\cdot}4$.

Fig. 11. Comparison of specimen results for long plates of constant and linearly varying thickness. Sides and ends clamped, $a/b_1 = 4$, $b_2/b_1 = 0{\cdot}4$.

Fig. 12. Specimen results for simply-supported plates, $a/b_1 = 2$, $b_2/b_1 = 0{\cdot}4$.

3.4. *Discussion of Results.*

3.4.1. *Comparison of one-function and two-function analyses.*—If the results of the two-function analyses plotted in Figs. 2 to 9 are compared with the corresponding results of single-function analyses, the following observations can be made.

(i) *Deflections.*—The maximum deflection results are virtually indistinguishable except for the shortest plates where differences of up to 2% occur.

(ii) *Stresses.*—When the maximum von Mises stress is not at the ends of the plate, the results of the two analyses converge as the length of the plate is increased. When a/b_1 is greater than 2 the difference in the results is less than 3% for a plate of constant thickness with clamped sides and is less than 1% for all the other examples calculated. When the maximum von Mises stress is at either end of the plate, the results, which do not converge as the length of the plate is increased, differ by

up to 3% for plates of constant thickness and $4\frac{1}{2}\%$ for plates with thickness proportional to width. The two-function analyses can be used however on plates sufficiently long for the stress distribution at the ends under this loading to depend purely on the angle of taper and not on the length of the plate.

3.4.2. *Optimum thickness variation.*—If a clamped plate such that $a/b_1 = 4$ and $b_2/b_1 = 0{\cdot}4$ is designed to a maximum stress specification under uniform load, a weight saving of the order of 14% is obtained by using the optimum linear thickness variation rather than a constant thickness. This confirms the usefulness of the optimum thickness variation for a plate under uniform loading.

NOTATION

Suffices 1 and 2 indicate values at $x = 0$ and $x = a$ respectively.

a, b — Length and width of plate

t — Plate thickness

x, y — Cartesian co-ordinates

w — Deflection

$\overline{w}$ — Maximum value of w

$\rho = \dfrac{b_2}{b_1} - 1$

$\mu = \dfrac{a}{b_1}$

$X = 1 + \rho \dfrac{x}{a}$

$Y = \dfrac{2y}{b_1}$

$W = \dfrac{w}{a}$

$\theta = \dfrac{Y}{X}$

E — Young's modulus

ν — Poisson's ratio (taken as 0·3 in computations)

D — Flexural rigidity $= Et^3/12(1-\nu^2)$

q — Normal loading

q_0, α, β — $q = q_0\alpha(X)\beta(\theta)$ where α and β are dimensionless functions

$R = \dfrac{q_0}{E}\left(\dfrac{b_1}{t_1}\right)^3$

$\sigma_x, \sigma_y, \tau_{xy}$ — Stresses

σ_f — Von Mises stress

$\overline{\sigma}_f$ — Maximum value of σ_f

M_x, M_y, M_{xy} — Bending and twisting moments per unit length

r — Index such that $D = D_1X^r$

v — Index such that $\alpha = X^v$

f_j — Unspecified function of X

NOTATION—*continued*

Φ_j	Known function of θ
$\Psi_j = \int_{-1}^{+1} \beta\Phi_j \, d\theta$	
p_{jki}	Defined by equations (9)
l_{jki}, m_{jk}, s_{jki}	Defined by equations (10)
λ_i	Indices in complementary function in equation (14)
$F_i(X)$	Particular integral
$h_{jk}(\lambda)$	Defined by equation (13)
Δ	Determinant of h_{jk} terms
A_i, B_i	Arbitrary constants in equations (14)
T	Work done by normal loading
U	Strain energy of bending
∇^2	Laplacian operator
∇^4	Biharmonic operator.

REFERENCES

No.	*Author*	*Title, etc.*
1	L. V. Kantorovich and V. I. Krylov	*Approximate methods of higher analysis.* Chapter 4. English translation by C. D. Benster of 3rd Russian edition. Noordhoff, 1958.
2	S. P. Timoshenko and S. Woinowsky-Krieger	*Theory of plates and shells.* Chapters 4 and 10, 2nd edition, McGraw-Hill, 1959.
3	M. L. Williams	Surface stress singularities resulting from various boundary conditions in angular corners of plates under bending. Proc. 1st U.S. Nat. Congress of Applied Mech., A.S.M.E., pp. 325 to 329. 1952.
4	G. G. Pope	The buckling of plates tapered in planform. A.R.C. R. & M. 3324. April, 1962.

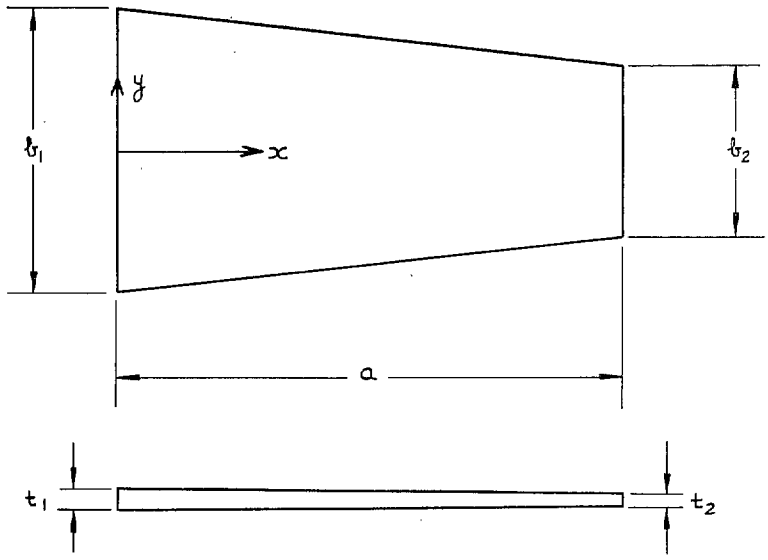

FIG. 1. Axes and notation.

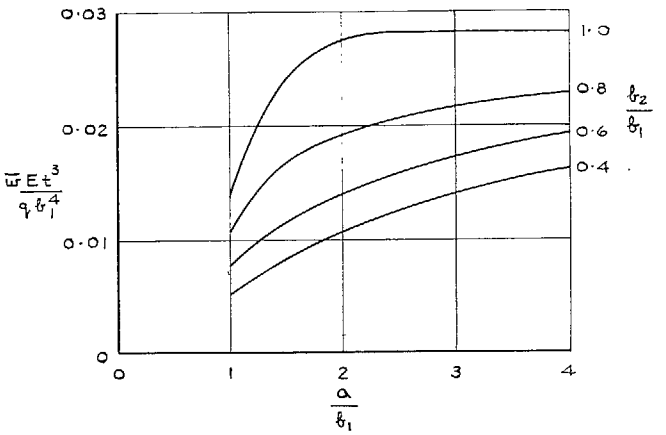

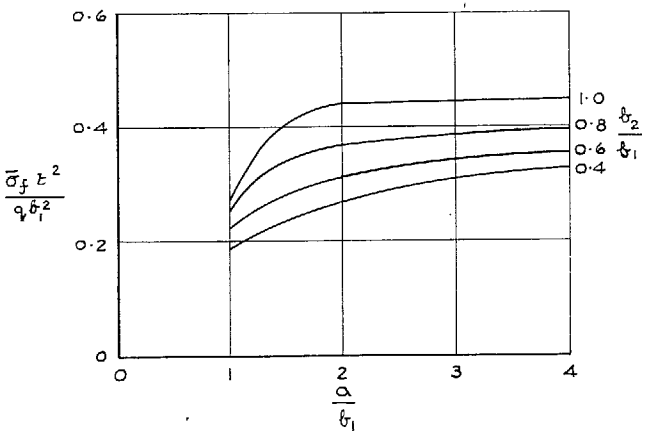

FIG. 2. Curves of maximum deflection and maximum σ_f. Sides and ends clamped, thickness constant.

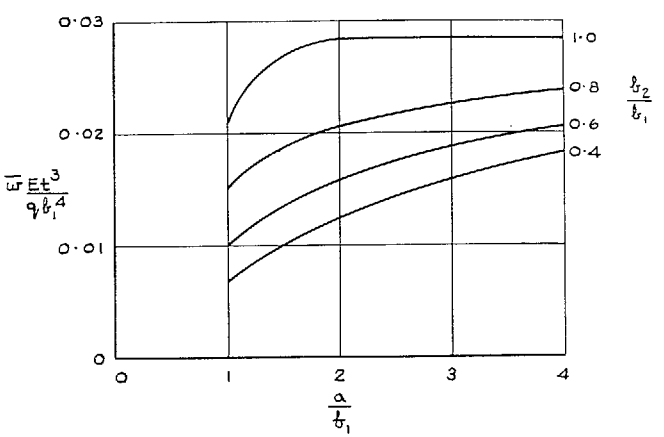

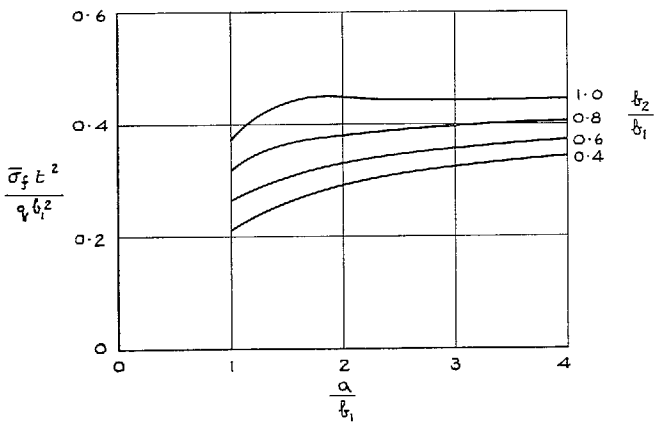

FIG. 3. Curves of maximum deflection and maximum σ_f. Sides clamped, ends simply-supported, thickness constant.

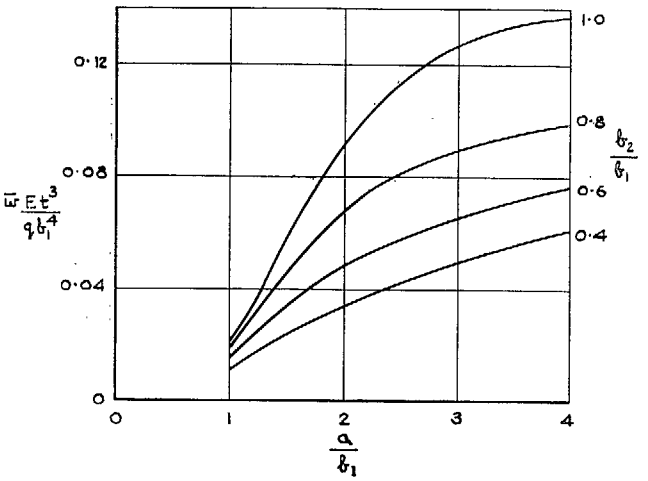

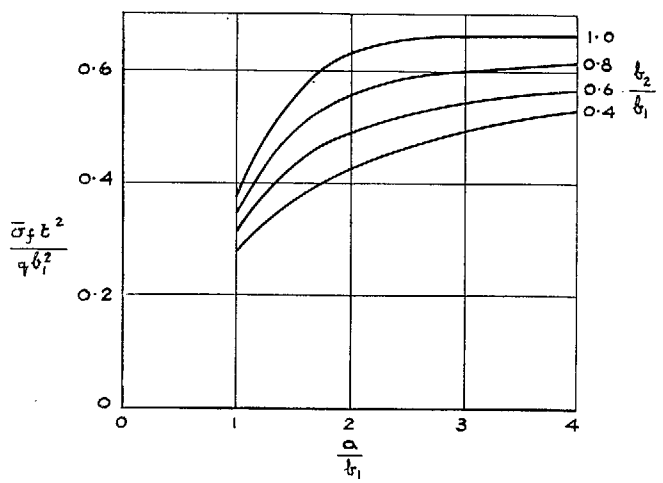

FIG. 4. Curves of maximum deflection and maximum σ_f. Sides simply-supported, ends clamped, thickness constant.

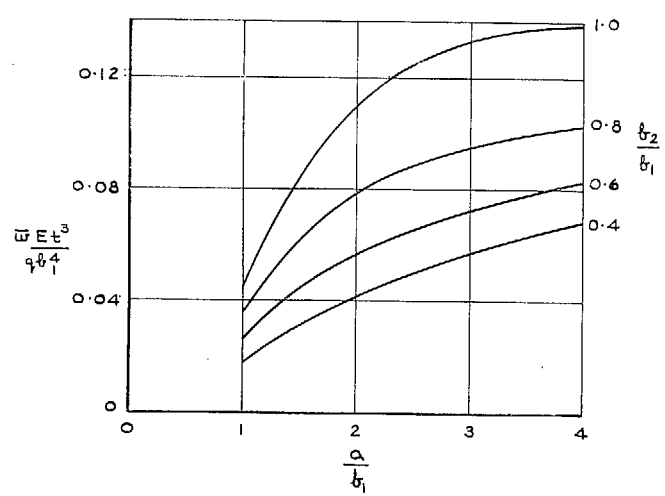

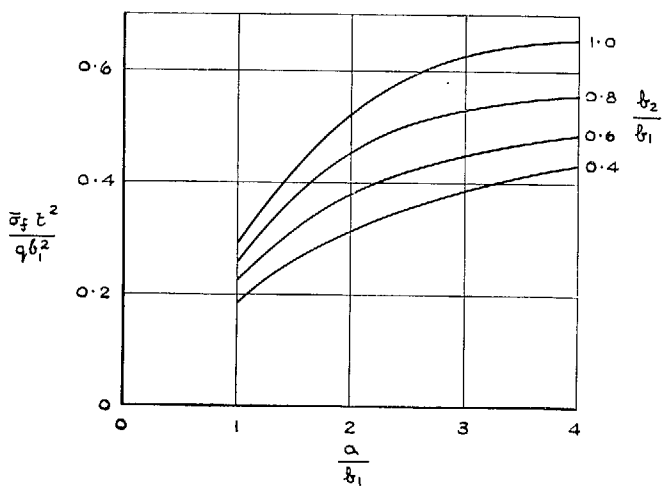

FIG. 5. Curves of maximum deflection and maximum σ_f. Sides and ends simply-supported, thickness constant.

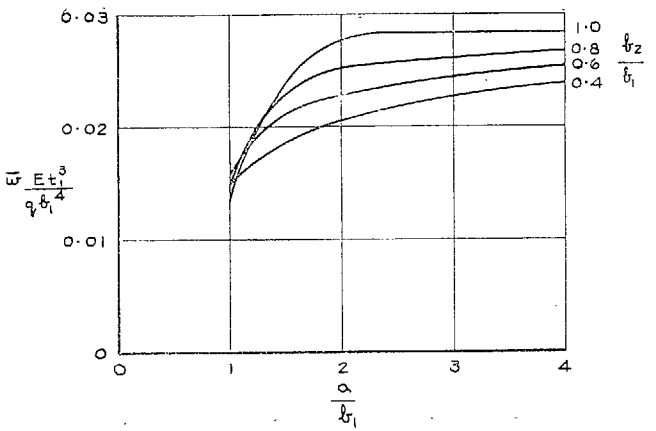

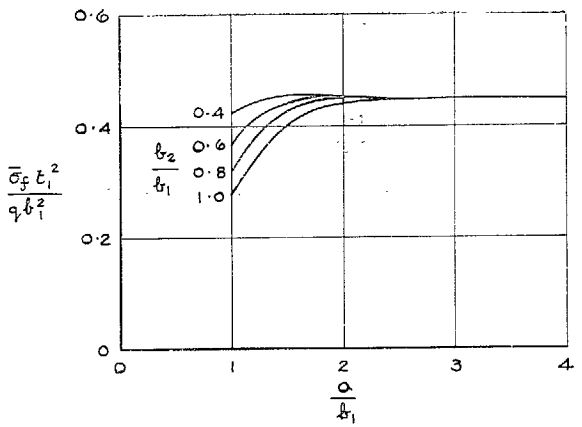

FIG. 6. Curves of maximum deflection and maximum σ_f. Sides and ends clamped, thickness proportional to width.

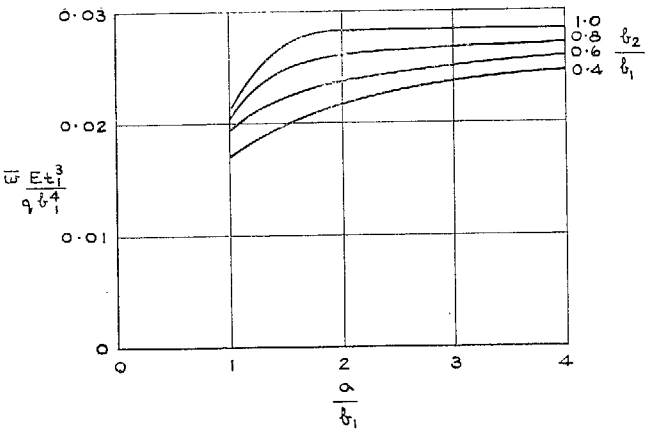

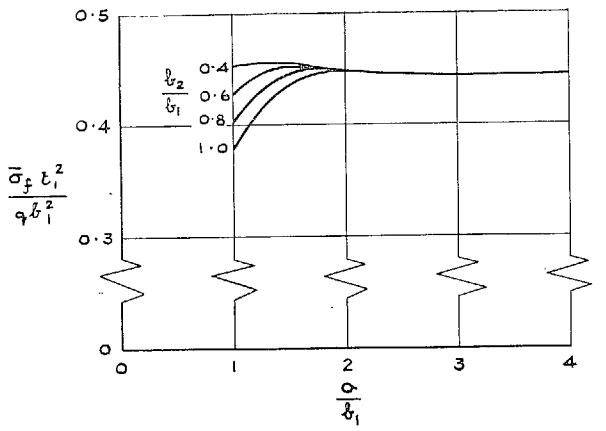

FIG. 7. Curves of maximum deflection and maximum σ_f. Sides clamped, ends simply-supported, thickness proportional to width.

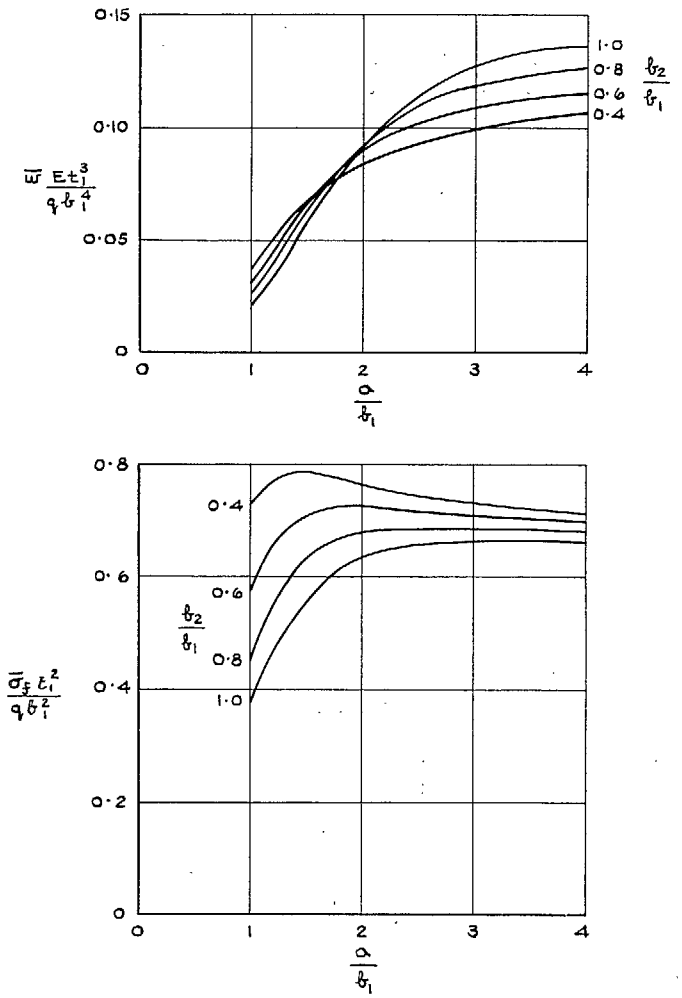

FIG. 8. Curves of maximum deflection and maximum σ_f. Sides simply-supported, ends clamped, thickness proportional to width.

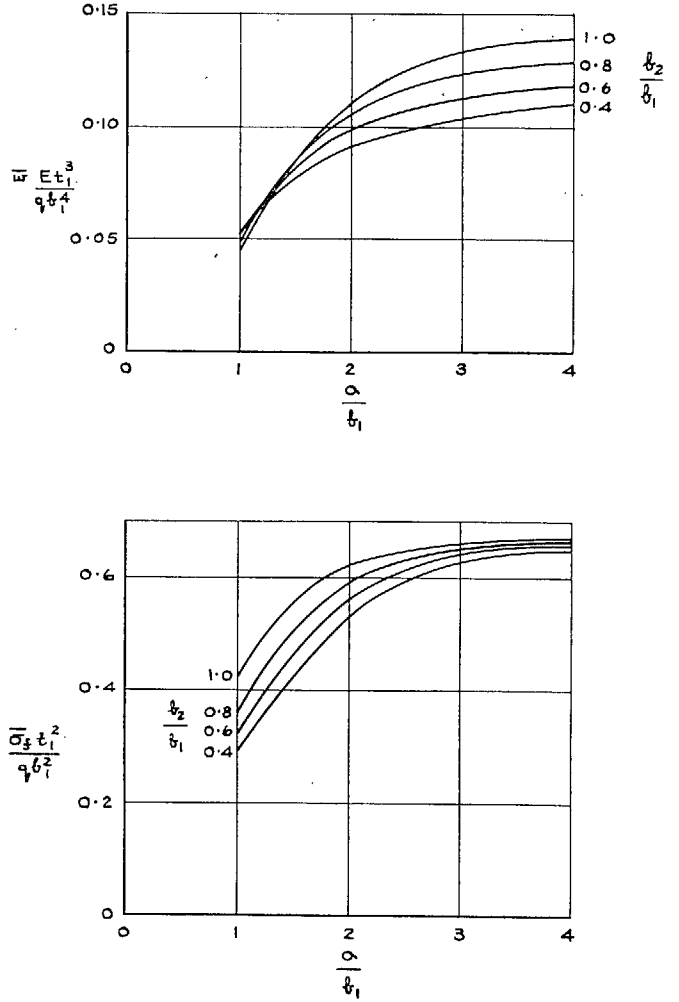

FIG. 9. Curves of maximum deflection and maximum σ_f. Sides and ends simply-supported, thickness proportional to width.

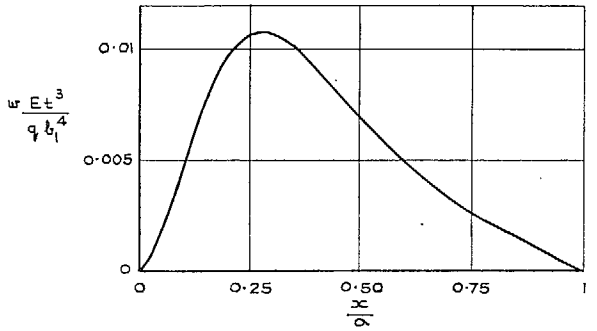

DEFLECTION OF CENTRE-LINE. RESULTS OF THE TWO ANALYSES ARE INDISTINGUISHABLE.

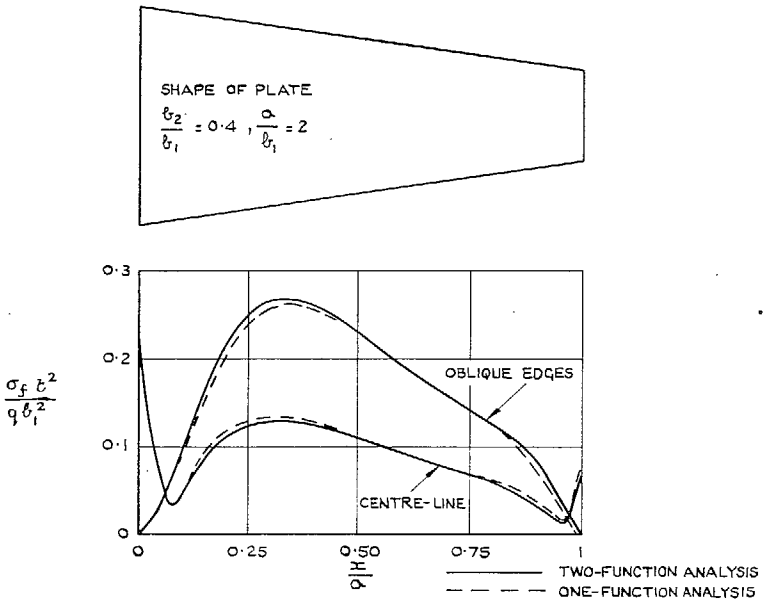

VON MISES STRESS ON SURFACE OF PLATE.

FIG. 10. Comparison of specimen results of the two analyses. Sides and ends clamped, thickness constant.

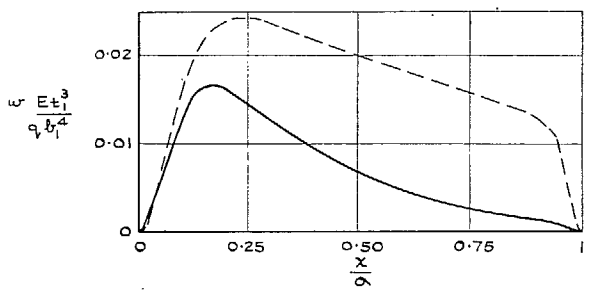

DEFLECTION OF CENTRE-LINE.

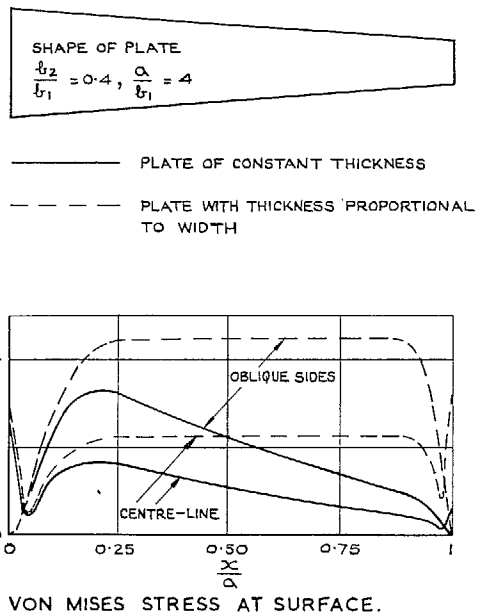

VON MISES STRESS AT SURFACE.

FIG. 11. Comparison of specimen results for long plates with thickness constant or proportional to width. Sides and ends clamped.

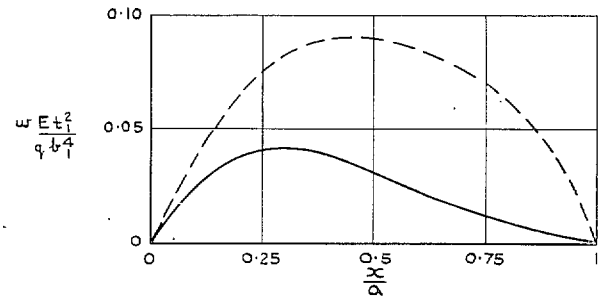

DEFLECTION OF CENTRE-LINE.

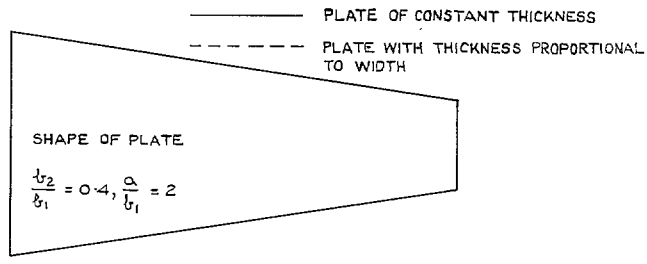

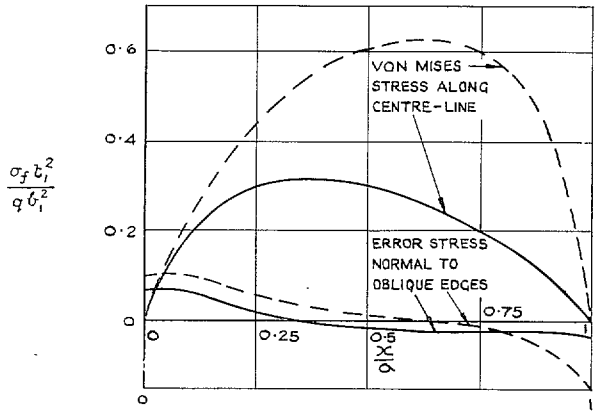

STRESSES AT SURFACE OF PLATE.

FIG. 12. Specimen results of two-function analysis of simply-supported plate.

(87122) Wt. 64/1857 K.5 6/63 Hw.

Publications of the Aeronautical Research Council

ANNUAL TECHNICAL REPORTS OF THE AERONAUTICAL RESEARCH COUNCIL (BOUND VOLUMES)

1942 Vol. I. Aero and Hydrodynamics, Aerofoils, Airscrews, Engines. 75*s.* (post 2*s.* 9*d.*)
Vol. II. Noise, Parachutes, Stability and Control, Structures, Vibration, Wind Tunnels. 47*s.* 6*d.* (post 2*s.* 3*d.*)

1943 Vol. I. Aerodynamics, Aerofoils, Airscrews. 80*s.* (post 2*s.* 6*d.*)
Vol. II. Engines, Flutter, Materials, Parachutes, Performance, Stability and Control, Structures. 90*s.* (post 2*s.* 9*d.*)

1944 Vol. I. Aero and Hydrodynamics, Aerofoils, Aircraft, Airscrews, Controls. 84*s.* (post 3*s.*)
Vol. II. Flutter and Vibration, Materials, Miscellaneous, Navigation, Parachutes, Performance, Plates and Panels, Stability, Structures, Test Equipment, Wind Tunnels. 84*s.* (post 3*s.*)

1945 Vol. I. Aero and Hydrodynamics, Aerofoils. 130*s.* (post 3*s.* 6*d.*)
Vol. II. Aircraft, Airscrews, Controls. 130*s.* (post 3*s.* 6*d.*)
Vol. III. Flutter and Vibration, Instruments, Miscellaneous, Parachutes, Plates and Panels, Propulsion. 130*s.* (post 3*s.* 3*d.*)
Vol. IV. Stability, Structures, Wind Tunnels, Wind Tunnel Technique. 130*s.* (post 3*s.* 3*d.*)

1946 Vol. I. Accidents, Aerodynamics, Aerofoils and Hydrofoils. 168*s.* (post 3*s.* 9*d.*)
Vol. II. Airscrews, Cabin Cooling, Chemical Hazards, Controls, Flames, Flutter, Helicopters, Instruments and Instrumentation, Interference, Jets, Miscellaneous, Parachutes. 168*s.* (post 3*s.* 3*d.*)
Vol. III. Performance, Propulsion, Seaplanes, Stability, Structures, Wind Tunnels. 168*s.* (post 3*s.* 6*d.*)

1947 Vol. I. Aerodynamics, Aerofoils, Aircraft. 168*s.* (post 3*s.* 9*d.*)
Vol. II. Airscrews and Rotors, Controls, Flutter, Materials, Miscellaneous, Parachutes, Propulsion, Seaplanes, Stability, Structures, Take-off and Landing. 168*s.* (post 3*s.* 9*d.*)

1948 Vol. I. Aerodynamics, Aerofoils, Aircraft, Airscrews, Controls, Flutter and Vibration, Helicopters, Instruments, Propulsion, Seaplane, Stability, Structures, Wind Tunnels. 130*s.* (post 3*s.* 3*d.*)
Vol. II. Aerodynamics, Aerofoils, Aircraft, Airscrews, Controls, Flutter and Vibration, Helicopters, Instruments, Propulsion, Seaplane, Stability, Structures, Wind Tunnels. 110*s.* (post 3*s.* 3*d.*)

Special Volumes

Vol. I. Aero and Hydrodynamics, Aerofoils, Controls, Flutter, Kites, Parachutes, Performance, Propulsion, Stability. 126*s.* (post 3*s.*)
Vol. II. Aero and Hydrodynamics, Aerofoils, Airscrews, Controls, Flutter, Materials, Miscellaneous, Parachutes, Propulsion, Stability, Structures. 147*s.* (post 3*s.*)
Vol. III. Aero and Hydrodynamics, Aerofoils, Airscrews, Controls, Flutter, Kites, Miscellaneous, Parachutes, Propulsion, Seaplanes, Stability, Structures, Test Equipment. 189*s.* (post 3*s.* 9*d.*)

Reviews of the Aeronautical Research Council

1939–48 3*s.* (post 6*d.*) 1949–54 5*s.* (post 5*d.*)

Index to all Reports and Memoranda published in the Annual Technical Reports

1909–1947 R. & M. 2600 (out of print)

Indexes to the Reports and Memoranda of the Aeronautical Research Council

Between Nos. 2351–2449	R. & M. No. 2450	2*s.* (post 3*d.*)
Between Nos. 2451–2549	R. & M. No. 2550	2*s.* 6*d.* (post 3*d.*)
Between Nos. 2551–2649	R. & M. No. 2650	2*s.* 6*d.* (post 3*d.*)
Between Nos. 2651–2749	R. & M. No. 2750	2*s.* 6*d.* (post 3*d.*)
Between Nos. 2751–2849	R. & M. No. 2850	2*s.* 6*d.* (post 3*d.*)
Between Nos. 2851–2949	R. & M. No. 2950	3*s.* (post 3*d.*)
Between Nos. 2951–3049	R. & M. No. 3050	3*s.* 6*d.* (post 3*d.*)
Between Nos. 3051–3149	R. & M. No. 3150	3*s.* 6*d.* (post 3*d.*)

HER MAJESTY'S STATIONERY OFFICE

from the addresses overleaf

Printed and published by
HER MAJESTY'S STATIONERY OFFICE

To be purchased from
York House, Kingsway, London W.C.2
423 Oxford Street, London W.1
13A Castle Street, Edinburgh 2
109 St. Mary Street, Cardiff
39 King Street, Manchester 2
50 Fairfax Street, Bristol 1
35 Smallbrook, Ringway, Birmingham 5
80 Chichester Street, Belfast 1
or through any bookseller

Printed in England

S.O. Code No. 23-3325